RSC Advances

PAPER

View Article Online
View Journal | View Issue

Cite this: *RSC Adv.*, 2024, **14**, 18161

Investigation of the effects of irradiation and aging on the tribological behavior of ultra-high molecular weight polyethylene/graphene oxide composites under water lubrication

Guodong Huang, *[a] Weiwen Lv,[a] Yaowu Zhu,[a] Zhigang Zhang,[a] Xuxing Jin,[a] Haowu Liu,[a] Tao Zhang, *[a] Fei Yang,[a] Min Lu[a] and Yongwu Zhao[b]

Ultra-high molecular weight polyethylene/graphene oxide (PE-UHMW/GO) composites have demonstrated potential in artificial joint applications. The tribological behavior of irradiated PE-UHMW/GO composites under water lubrication remained unclear, which limited their application range. In this study, the PE-UHMW/GO composites were gamma irradiated at 100 KGy in a vacuum and subsequently aged at 80 °C for 21 days in air. We assessed their water absorption, and mechanical and tribological properties post-treatment. Notably, gamma irradiation markedly enhanced the mechanical and tribological performance of PE-UHMW/GO composites. Irradiated composites had a 6.11% increase in compressive strength and a 25.72% increase in yield strength compared to unirradiated composites. Additionally, under water lubrication, the irradiated composites showed improved wear resistance and a reduced friction coefficient. The irradiation enhancement can be attributed to the irradiation-induced strengthening of the interface bonding between GO and PE-UHMW. Conversely, accelerated aging led to oxidative degradation, negatively impacting these properties. Aged composites exhibited lower compressive and yield strengths, higher friction coefficients, and diminished anti-wear properties compared to the irradiated composites. The wear mechanism evolved from predominantly fatigue wear in irradiated PE-UHMW/GO to a mix of abrasive and fatigue wear post-aging. While GO and aging influenced water absorption, irradiation had a minimal effect. These insights significantly contribute to the application potential of irradiated PE-UHMW/GO composites in artificial joints.

Received 15th February 2024
Accepted 27th May 2024

DOI: 10.1039/d4ra01156b

rsc.li/rsc-advances

1. Introduction

Ultra-high molecular weight polyethylene (PE-UHMW) is recognized as a crucial material for biomedical applications.[1,2] PE-UHMW possesses superior characteristics, including a lower friction coefficient,[3] high chemical inertness,[4] good biocompatibility,[5] and excellent wear resistance.[6] Market prediction estimates that the market valuation of medical-grade PE-UHMW will reach US$2.39 billion by 2024, with an expected compound annual growth rate (CAGR) of 5.1% from 2015 to 2024.[7] In the field of orthopedic surgery, PE-UHMW has already been extensively used as the load-bearing material in artificial joint replacement. However, the prolonged use of PE-UHMW in artificial joints can generate wear debris, which may cause inflammation and osteolysis, and ultimately lead to the failure of artificial joints. Consequently, it is crucial to enhance the anti-wear properties of PE-UHMW. Currently, various techniques have been developed to improve the wear resistance of PE-UHMW. Notably, the addition of reinforcement particles and the use of irradiation are two of the most important techniques.

The incorporation of reinforcing particles into the PE-UHMW matrix improves the mechanical properties and wear resistance of PE-UHMW. Currently, widely employed reinforcing particles include carbon nanofibers (CNFs),[8] carbon nanotubes (CNTs),[9] graphene,[10] graphite,[11] hard particles[12] and graphene oxide (GO).[13–15] Particularly, GO, as a graphene derivative, has attracted considerable attention for its distinctive two-dimensional (2D) network, high specific surface area, and excellent mechanical performance. Compared to graphene, GO contains numerous oxygen-containing functional groups, such as carboxyl, hydroxyl, epoxy, and other oxygen-containing functional groups, enabling better dispersion into the polymer matrix.[16] Therefore, GO is deemed an ideal additive for PE-UHMW. Extensive research has been conducted on PE-UHMW/GO composites. Chen *et al.*[13] successfully prepared PE-UHMW/GO composites through ultrasonic dispersion and hot-pressing. The composites displayed significant increases in microhardness and optimal tensile

[a]*School of Mechanical Engineering, Wuxi Institute of Technology, Wuxi 214121, Jiangsu, China. E-mail: huanggd@wxit.edu.cn; zhangt@wxit.edu.cn*
[b]*School of Mechanical Engineering, Jiangnan University, Wuxi 214122, Jiangsu, China*

strength with 0.5 wt% GO. Similarly, Pang *et al.*[17] demonstrated enhancement in both mechanical and thermal properties by incorporating GO. Tai *et al.*[18] found that adding GO efficiently improved the wear resistance of PE-UHMW/GO composites under dry friction conditions, with consistent results under deionized water and normal saline lubrication conditions.[19] Suner *et al.*[20] analyzed the effect of GO content on PE-UHMW/GO composites, finding that 0.5 wt% GO was the optimal addition amount for enhanced mechanical and wear resistance properties. The cumulative findings from these studies suggest that GO significantly improves the mechanical and wear resistance properties of PE-UHMW.

Irradiation technology is an alternative approach for polymer modification. PE-UHMW commonly undergoes gamma irradiation when used as artificial joint materials. This technique not only sterilizes PE-UHMW materials,[21] but also improves their performance. Exposure of PE-UHMW to gamma irradiation leads to the generation of free radicals the breaking of carbon–carbon (C–C) bonds and hydrogen–carbon (C–H) bonds within its molecular chains.[22] In the amorphous phase of PE-UHMW, the majority of free radicals are recombined with each other to form crosslinks, thereby enhancing anti-wear properties. However, in the crystalline phase of PE-UHMW, residual free radicals react directly with oxygen to generate hydroperoxides in the presence of air, significantly degrading the mechanical and anti-wear properties. Therefore, free radical scavengers such as Vitamin E[23] and multi-walled carbon nanotubes[24] are incorporated into the PE-UHMW matrix to eliminate residual free radicals and efficiently restrict oxidation reactions.

Although some studies have delved into the wear resistance and mechanical properties of the PE-UHMW/GO composites, these investigations remain insufficient for their application in artificial joints. It is imperative to explore the impact of irradiation and aging on these composites. However, to the best of our knowledge, the effects of gamma irradiation and aging on the tribological properties of PE-UHMW/GO composites, especially under water lubrication conditions, have been scarcely investigated. In this study, high-performance PE-UHMW/GO composites were prepared. The composites underwent irradiation and accelerated aging treatments. Their mechanical performance and the tribological properties under water lubrication conditions were systematically analyzed.

2. Experimental

2.1 Materials

The GUR1050 PE-UHMW powder used in this study was obtained from Ticona/Celanese (Dallas, TX, USA). The 325-mesh high-purity graphite powder, with a purity of 99.9%, was acquired from Qingdao Jin-Ri-Lai Graphite Co., Ltd (Qingdao, China). All remaining chemical reagents (analytica pure) were procured from Sinopharm Chemical Reagent Co., Ltd (Shanghai China).

2.2 Preparation of PE-UHMW/GO composites

GO was prepared using the modified Hummers process,[25] starting with pure graphite powder. Prior investigations[20] suggested that the ideal proportion of GO to be incorporated into PE-UHMW was 0.5 wt%. Consequently, in this study, a concentration of 0.5 wt% GO was added to PE-UHMW.

The preparation of PE-UHMW/GO composites was as follows: 0.5 g GO was initially dispersed in 500 mL alcohol using mild ultrasound for 30 minutes, ensuring an exfoliated and homogeneous dispersion. Gradually, 99.5 g PE-UHMW powder was introduced into the GO suspension, followed by an additional 40 minutes of ultrasonication to guarantee a uniform suspension. The composite powder was then subjected to a 6 hours drying period at 60 °C in a water bath. The resulting composite powder underwent ball milling at a velocity of 400 revolutions per minute for 2 hours. The composite powder underwent preliminary compression within a steel mold under a pressure of 15 MPa for 15 minutes. Subsequently, a 2 hours heat treatment at 200 °C in an air oven, without applying pressure, was carried out. The composite powder was further pressed at 10 MPa until it reached room temperature in the surrounding atmosphere. Through this series of meticulous procedures, the PE-UHMW/GO composites were successfully prepared.

PE-UHMW and PE-UHMW/GO composites were hermetically sealed in aluminum foil and irradiated at room temperature with cobalt-60 gamma rays at Wuxi EL PONT Radiation Technology Co., Ltd (Wuxi, China). The cumulative irradiation dosage was 100 kGy, with an irradiation rate of 0.5 kGy h^{-1}. In accordance with ASTM F2003-00, the irradiated samples were aged in a hot-air oven at 80 °C for 21 days.

2.3 Characterization

The surface morphology of GO was evaluated using a CSPM5000 atomic force microscope in tapping mode. The AFM was manufactured by Benyuan in Guangzhou, China. The sample preparation involved the following steps: one milligram of GO was dissolved in 400 mL of deionized water and sonicated for 40 minutes to ensure uniform dispersion. Subsequently, 0.1 mL of the GO solution was pipetted onto the surface of the silicon wafer and dried at 60 °C in a vacuum drying oven.

In order to analyze the dispersion of GO within the PE-UHMW matrix, Transmission Electron Microscopy (TEM), specifically the JEM-2100plus model from Japan, was utilized. The TEM sample preparation comprised a series of steps. Initially, 200 μm sections from both virgin PE-UHMW and PE-UHMW/GO composites were stained using 99% chlorosulphonic acid at 60 °C for 5 hours. Subsequently, the specimens were cleaned with acetone at 0 °C, and then rinsed with deionized water. After chemical treatment, they were dried for an hour at a temperature of 60 °C. Following that, they were immersed in epoxy and allowed to solidify at 60 °C for 48 hours. Using a diamond knife, thin sections with a thickness of approximately 100 nm were meticulously cut and affixed onto carbon grids for TEM analysis.

Scanning electron microscope (SEM) was utilized to investigate the surface morphology of GO and the wear surfaces of the composites. This investigation used three distinct SEM instruments: HITACHI SU1510 (Hitachi, Tokyo, Japan), Zeiss SIGMA (Zeiss, Oberkochen, Germany), and ZEISS-Merlin Compact (Zeiss, Oberkochen, Germany). The preparation of GO for SEM

analysis followed the same procedure as employed for AFM. All samples were gold-sprayed for 3 minutes and then placed on a rotation stage for SEM analysis.

The functional groups in GO was examined using Bruker Corporation's Alpha-Transmittance Fourier-Transform Infrared (FT-IR) spectrometer, situated in Germany. FT-IR spectroscopy was recorded in the wavenumber range of 600–4000 cm^{-1}.

2.4 Water sorption test

The water sorption test was executed following the ISO62-2008 standard. The test process is described below. The PE-UHMW/GO composites were cut into uniform pieces (70.00 mm × 70.00 mm × 2.05 mm), and their weight (m_1) was measured using an XS205DU electronic balance (Mettler Toledo, Greifensee, Switzerland). Subsequently, the samples were immersed in deionized water at 23 °C for 24 hours. After this immersion period, test samples were removed from the water, excess moisture was quickly blotted with filter paper, and the samples were promptly re-weighted (m_2). Consequently, the water absorption rate (c) could be calculated using the formula (1) below. Each sample was measured three times, and the average value and standard deviation were calculated.

$$c = \frac{m_2 - m_1}{m_2} \times 100\% \quad (1)$$

2.5 Compressive test

The uniaxial compressive test was performed using a universal mechanical testing machine (WDW-100E, Jinan Shi-Jing Testing Machine Co., Ltd, Jinan, China). The samples were cut into cubes with dimensions of 15.80 mm in thickness, 10.00 mm in length, and 6.20 mm in width. The compressive rate was maintained at 2 mm min^{-1} until the sample reached a compressive strain of 25%. Each sample type underwent three measurements.

2.6 Tribological test

The tribological behavior of the composites was evaluated using a Multi-Function MFT-5000 tribometer (Rtec Instruments, USA). Fig. 1 depicts the schematic diagram of the tribological test conducted under lubrication conditions. The MFT-5000 tribometer measured the friction coefficient (μ) during linear reciprocating motion in the ball-on-plate mode. The reciprocating frequency was set to 1 Hz, and the friction stroke (B) was set to 10.00 mm. The wear test last for 3600 seconds.

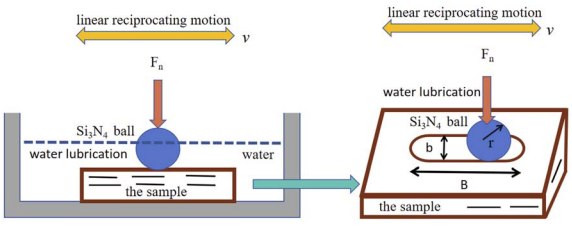

Fig. 1 The schematic diagram of the friction and wear testing process under water lubrication.

Throughout the friction process, the normal force (F_n) of 15N was applied to a Si_3N_4 ball, serving as the frictional counterpart, with a radius (r) of 2.50 mm. The automatic recording of the friction force (F_f) led to the subsequent calculation of the friction coefficient (μ) using the provided eqn (2). Each sample was measured three times, and the average friction coefficient were calculated. After the friction test, all samples were washed with acetone and dried at 30 °C for 6 hours. The wear width (b) and length (B) were measured with a white light interferometer (UP-3000 Rtec Instruments, USA). The wear volume (V) was calculated using eqn (3). The wear rate (K) was calculated using eqn (4), where L was the total distance traveled by the ball. The average wear rate was calculated according to these measurements.

$$\mu = \frac{F_f}{F_n} \quad (2)$$

$$V = B\left[\frac{\pi r^2}{180}\arcsin\frac{b}{2r} - \frac{b}{2}\sqrt{r^2 - \frac{b^2}{4}}\right] \quad (3)$$

$$K = \frac{V}{F_n \times L} \quad (4)$$

3. Results and discussion

3.1 The morphological characterization of GO

Fig. 2 depicts the morphological characterization of the self-prepared GO. Owing to its large surface area, GO trended to self-assemble into multilayered clusters. The TEM image of GO (Fig. 2(a)) exhibited a surface with conspicuous wrinkles and folds. SEM observation (Fig. 2(b)) showed GO with an irregular sheet shape structure with varying dimensions, typically ranging from a few micrometers. The surface of GO appeared rough and uneven, displaying numerous wrinkles and folds originating from defects in the carbon atoms of GO. The epoxy groups on the surface of GO were volatile and easily decomposed into carbon dioxide (CO_2)[26] upon exposure to heat, thereby generating vacancy defects. The wrinkles and folds were pronounced in areas where the epoxy groups aggregated. The interaction of polymers with GO induced more wrinkles and folds on the GO surface, establishing a strong mechanical interlock[27] with the polymer and enhancing the transfer of forces within the polymer. The thickness of GO, as measured from the AFM image (Fig. 2(c) and (d)), was approximately 1.34 nm. This measurement exceeded the ideal monolayer graphene thickness of 0.34 nm.[28] However, literature reports suggest the monolayer thickness of GO around 1 nm.[29] In this study, the prepared GO consisted primarily of monolayers or few-layer structures (oligolayers), influenced by wrinkles and folds. The particle size of GO ranged from 0.10 to 10.00 μm.

The presence of a significant amount of oxygen-containing functional groups in GO can be observed in Fig. 2(e). The C=C stretching vibrational peak with sp^2 structure was located at 1624 cm^{-1}. A rather broad absorption peak, centered around 3400 cm^{-1}, likely stemmed from the presence of non-reduced

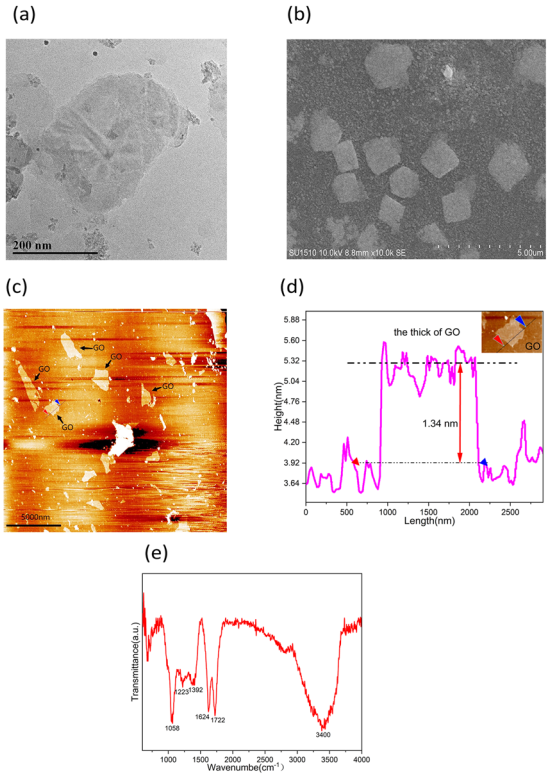

Fig. 2 Morphological characterization of GO: (a) TEM image of GO, (b) SEM image of GO, (c) AFM image of GO, (d) the thick of GO, (e) FTIR spectroscopy of GO.

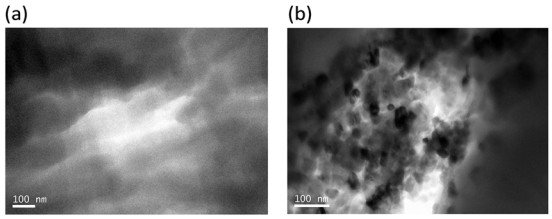

Fig. 3 TEM images: (a) PE-UHMW, (b) PE-UHMW/GO composites.

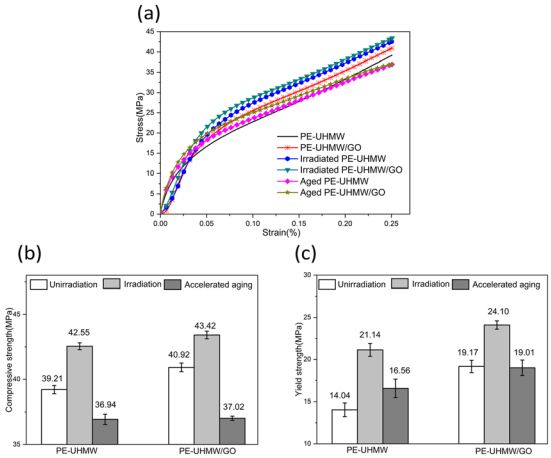

Fig. 4 Impressive properties of different treated PE-UHMW and PE-UHMW/GO composites: (a) compressive stress–strain curve, (b) compressive strength, (c) yield strength.

hydroxyl groups (–OH) and the absorption of water molecules. The observed absorption peak at approximately 1722 cm^{-1} signified the vibrational mode of the carbonyl (C═O) group, implying the oxidation of edge carbon leading to the formation of C(═O)–OH. Moreover, the absorption peak around 1392 cm^{-1} was ascribed to the bending vibrations of hydroxyl (–OH) groups within the GO framework structures. The absorption peak detected in proximity to 1223 cm^{-1} was associated with the vibrational modes of the C–OH bond, whereas the peak around 1058 cm^{-1} hinted at the existence of C–O vibrational modes. The presence of polar oxygen-containing functional groups facilitated the establishment of hydrogen bonds with water molecules, contributing to an enhanced hydrophilic nature of GO.

3.2 The dispersibility of GO in the composites

The dispersion of fillers in composite materials influences their overall performance. The TEM images of pure PE-UHMW and PE-UHMW/GO composites were shown in Fig. 3. Significantly, GO exhibited better dispersibility within the PE-UHMW matrix. Compared to graphene, the ease of dispersing GO into the polymer matrix was due to its plentiful functional groups. Therefore, GO has the potential to enhance the performance of polymers.

3.3 Compressive properties of different treated composites

The mechanical properties of the composites have been affected by gamma irradiation and accelerated aging. The results of the uniaxial compressive test of the samples are presented in Fig. 4.

The compressive strength and yield strength were determined based on the results of the impressive stress–strain curve.

Incorporating a minor amount of GO greatly enhanced the mechanical properties of PE-UHMW, as shown in Fig. 4(b) and (c). The compressive strength and yield strength of PE-UHMW and PE-UHMW/GO were 39.21 MPa and 14.04 MPa, and 40.92 MPa and 19.17 MPa, respectively. The compressive strength and yield strength of PE-UHMW/GO composites increased by 4.36% and 36.54%, respectively, compared with pure PE-UHMW. The enhancing effect of GO can be attributed to its exceptional mechanical properties and two-dimensional network structure. GO exhibited a modulus of elasticity and tensile strength of approximately 230 GPa and 0.13 GPa,[30] respectively, surpassing those of the PE-UHMW matrix. The two-dimensional network structure of GO facilitated the effective transfer and distribution of external loads from the PE-UHMW matrix to the GO sheets. Wrinkles and folds in GO tightly attached to the PE-UHMW matrix, enhancing mechanical locking. Furthermore, the numerous functional groups in GO improved compatibility with the polymer, allowing more efficient transfer of interfacial forces within the polymer to GO.

Irradiation further improved the mechanical properties of the composites. The compressive strength and yield strength of PE-UHMW/GO and irradiated PE-UHMW/GO were 40.92 MPa and 19.17 MPa, and 43.42 MPa and 24.10 MPa, respectively. The irradiated PE-UHMW/GO exhibited a 6.11% increase in

compressive strength and a 25.72% increase in yield strength, compared to the unirradiated PE-UHMW/GO. Similar test results were also observed by Martinez *et al.*[24] in their study of irradiated PE-UHMW/MWNT. Typically, the crystalline nature of composites influences their mechanical characteristics. The irradiation increases the crystallinity of PE-UHMW due to the generation of numerous free radicals from the breakage of PE-UHMW molecular chains, which recombine with each other and form crosslinks. Huang *et al.*'s[31] investigation into the dfferential scanning calorimetry (DSC) results of composites verified this. Irradiation also affected GO, causing it to be reduced to reduced graphene oxide (rGO), generating unpaired electrons on the rGO plane. Interaction between rGO and the molecular chains or free radicals in PE-UHMW contributed to enhanced mechanical properties. Furthermore, rGO exhibited superior mechanical performance to GO,[32] implying its ability to bear more force in the matrix. The above analysis showed that irradiation significantly enhanced the mechanical properties of PE-UHMW/GO composites.

However, the aging process had a significant adverse effect on the mechanical properties of the composites. The average compressive strength and yield strength of aged PE-UHMW/GO were 37.02 MPa and 19.01 MPa, respectively. Compressive strength and yield strength of aged PE-UHMW/GO were reduced by 14.74% and 21.12%, respectively, compared to irradiated PE-UHMW/GO. This reduction can be attributed to thermo-oxidative degradation.[33] During the accelerated aging process, elevated temperatures expedited the internal diffusion of oxygen within the PE-UHMW, hastening the reaction with remaining free radicals to produce oxidation byproducts such as ketones, alcohols, and esters, among others.[33] These oxidation products directly led to the degradation of the composites' mechanical properties. However, aged PE-UHMW/GO displayed better mechanical properties than aged PE-UHMW, suggesting that irradiation and GO could mitigate the degradation of the mechanical properties of PE-UHMW.

3.4 Water sorption capacity of different treated composites

The water absorption rate of the specimens is presented in Table 1. The incorporation of GO significantly enhanced the water absorption of the composites. When compared to pure PE-UHMW, the water sorption of PE-UHMW/GO experienced a remarkable improvement of 507.69%, due to the exceptional hydrophilicity of GO. Notably, it was observed that irradiation had minimal impact on the water absorption of the composite.

Table 1 Water absorption rate of different treated PE-UHMW and PE-UHMW/GO composites

The sample	Water absorption rate c (%) (mean ± standard deviation)
PE-UHMW	0.0013 ± 0.00044
PE-UHMW/GO	0.0079 ± 0.0010
Irradiated PE-UHMW	0.0010 ± 0.00027
Irradiated PE-UHMW/GO	0.0073 ± 0.0012
Aged PE-UHMW	0.0026 ± 0.00062
Aged PE-UHMW/GO	0.023 ± 0.0066

However, aging resulted in a significant increase of 191.14% in water absorption of aged PE-UHMW/GO compared to PE-UHMW/GO composites. This phenomenon can be attributed to oxidative degradation, leading to the formation of oxygenation products on the surface of the composites. Furthermore, oxidation reduced the compactness of the polymer, rendering it more susceptible to the penetration of water molecules.

3.5 Friction and wear properties of different treated composites under water lubrication condition

Fig. 5 displays the friction and wear results of different treated samples under water-lubricated conditions. Fig. 5(a) illustrates the curve of the friction coefficients over time, revealing a consistent change trend for most samples, except for aged PE-UHMW/GO. In the initial stages (<600 s), the coefficient of friction for most samples gradually decreased over time, achieving stabilization after 300 seconds. However, the friction behavior of aged PE-UHMW/GO displayed distinct variations. Initially, the coefficient of friction experienced a gradual increase, reaching its peak values before 300 seconds. Subsequently, it immediately decreased, reaching its lowest value between 300 and 1200 seconds. Finally, after 1200 seconds, it gradually increase again, stabilizing after 2400 seconds. Fig. 5(b) displays the average friction coefficient of these samples.

According to Fig. 5(a) and (b), both GO and irradiation exerted significantly impacts the coefficient of friction. The average friction coefficients of PE-UHMW and PE-UHMW/GO were 0.0607 and 0.0536, respectively. The addition of GO efficiently reduced the coefficient of friction of PE-UHMW due to the hydrophilicity of GO. Additionally, irradiation also greatly improved friction properties. Irradiation caused the friction coefficient of PE-UHMW/GO to decrease from 0.0536 to 0.0423. The irradiation process resulted in the reduction of GO to rGO, which exhibited better lubrication properties.[34] However, after accelerated aging, the friction coefficient of PE-UHMW reached a minimum value of 0.0402. Unfortunately, aging failed to reduce the coefficient of

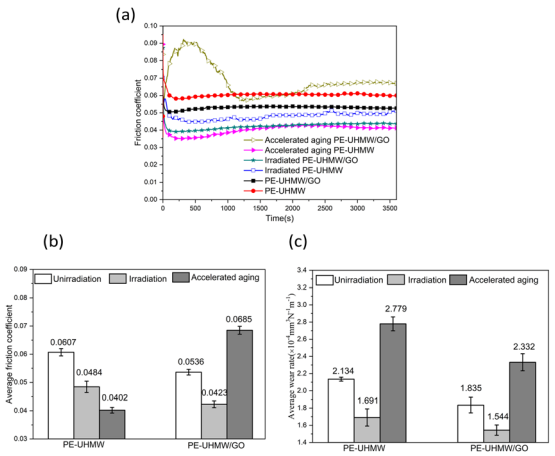

Fig. 5 Fiction and wear of different treated PE-UHMW and PE-UHMW/GO composites under lubrication with water: (a) friction coefficient *vs.* time curve, (b) average friction coefficient, (c) average wear rate.

friction in the PE-UHMW/GO composites. Instead, the average coefficient of friction reached a maximum value of 0.0685, indicating that aging resulted in a deterioration of friction properties. Oxidative degradation induced many bond scissions, weakening the interfacial binding force between GO and the PE-UHMW matrix. Consequently, numerous wear particles were easily generated, leading to three-body abrasion. As a result, aged PE-UHMW/GO had a higher friction coefficient.

The average wear rate of the composites is displayed in Fig. 5(c). In the presence of water, hydrophilic GO had a significant influence on the wear rate in the boundary lubrication regime. The wear rate of PE-UHMW was 2.134×10^{-4} mm^3 N^{-1} m^{-1}, while the wear rate of PE-UHMW/GO was measured at 1.835×10^{-4} mm^3 N^{-1} m^{-1}, demonstrating a 14.01% reduction compared to PE-UHMW. After irradiation, the wear rate of irradiated PE-UHMW/GO decreased to 1.544×10^{-4} mm^3 N^{-1} m^{-1}, showing a reduction of 8.69% compared to irradiated PE-UHMW. However, post-aging treatment, the wear rate of PE-UHMW reached the maximum value of 2.779×10^{-4} mm^3 N^{-1} m^{-1}. While, PE-UHMW/GO composites was measured at 2.332×10^{-4} mm^3 N^{-1} m^{-1}, exhibiting a notable 16.08% reduction compared to the wear rate of aged PE-UHMW. Based on the experiment results mentioned above, incorporating GO nanoparticles significantly enhanced the wear resistance of specimens. This enhancement can be attributed to two primary factors. Firstly, the addition of GO enhanced the mechanical properties of PE-UHMW, thereby increasing resistance to plastic deformation. Secondly, GO contributed to a reduction in the friction coefficient, consequently mitigating wear.

Irradiation further enhanced the wear resistance of the specimens under water-lubricated conditions. The wear rate of irradiated PE-UHMW/GO was measured at 1.544×10^{-4} mm^3 N^{-1} m^{-1}, showing a 15.86% reduction compared to PE-UHMW/GO. Similarly, the wear rate of irradiated PE-UHMW, recorded at 1.691×10^{-4} mm^3 N^{-1} m^{-1}, demonstrated a 20.76% decrease compared to PE-UHMW. Irradiation process increased crystallinity and mechanical properties, enhancing the compactness of the composites. This improvement effectively decreased water penetration and reduced plasticization.[35] Consequently, the wear rate of irradiated samples was lower than that of unirradiated counterparts.

During the aging process, free radicals within the PE-UHMW matrix reacted with oxygen to generate numerous oxidation products, reducing the mechanical properties of the specimen. These oxidation products were susceptible to hydrolysis reactions,[36] thereby accelerating the specimen's wear. Simultaneously, while the generated oxidation products increased the hydrophilicity of the specimen, they also reduced their density, facilitating easier water penetration and an increase in the water absorption rate. Consequently, the composites became more prone to abrasion, generating a large amount of abrasive debris under reciprocating stress, further aggravating the wear. Although aged PE-UHMW/GO exhibited a greater water absorption capacity compared to aged PE-UHMW, the wear rate of aged PE-UHMW/GO was lower than that of PE-UHMW, which was mainly attributed to the excellent mechanical properties of GO. It meant that GO had the role of protecting the matrix.

3.6 Wear morphology and wear mechanism of different treated composites

Fig. 6 displayed the SEM images (1000× magnification) of the worn surface of the samples. On the worn surface of virgin PE-UHMW, a certain number of minor cracks and fatigue spalling along the direction of frictional sliding (Fig. 6(a)). This occurrence was attributed to the wedging effect of water immersion expansion and the hydrostatic pressure of water, thereby initiating crack growth. As these cracks expanded and experienced the impact of water, material layers peeled away. In contrast, the wear surface of PE-UHMW/GO exhibited continuous material peeling perpendicular to the direction of friction (Fig. 6(b)). The incorporation of GO into the PE-UHMW matrix enhanced the material's water absorption capacity. Interfacial voids between GO and PE-UHMW facilitated the infiltration and dispersion of water molecules within these voids. Under conditions of reciprocating shear, these regions were susceptible to tearing and, subsequently, were removed by water flow, leading to extensive peeling. The wear mechanism observed in both PE-UHMW and PE-UHMW/GO was fatigue wear.

Irradiated PE-UHMW exhibited a reduction in the incidence of fatigue cracks on the wear surface compared to unirradiated PE-UHMW (Fig. 6(c)). However it displayed a substantial presence of furrows and scratches, accompanied by a significant amount of wear particles on the surface, indicating pronounced abrasive wear throughout the process. Irradiation enhanced the mechanical properties, resulting in improved resistance to fatigue wear and a marked reduction in fatigue cracks. The surface of irradiated PE-UHMW was easily oxidized, producing oxidative products that could readily undergo hydrolysis in water, leading to surface softening. A substantial number of furrows and scratches emerged as the convex surface of the ball traversed the specimen surface. After irradiation, a minor degree of fatigue spallings and cracks was observed on the wear surface of PE-UHMW/GO (Fig. 6(d)). Notably, irradiation had a profound impact on reducing fatigue wear. The irradiation process enhanced interfacial bonding between the matrix and GO, thereby improving the mechanical properties of the composites. Moreover, irradiation promoted internal densification of specimens, diminished internal voids, reduced water infiltration, and significantly curtailed the occurrence of extensive peeling. For irradiated PE-UHMW, the primary wear mechanism was abrasive wear, whereas for irradiated PE-UHMW/GO, it was fatigue wear.

Aged PE-UHMW showed minor fatigue spallings, cracks, and furrowings on the wear surface resulting from oxide deterioration (Fig. 6(e)). In contrast, the worn surface of aged PE-UHMW/GO displayed ripple-like undulations and furrows (Fig. 6(f)). The aging effect decreased the interfacial bonding between the matrix and GO.

Under the action of reciprocating shear, plastic deformation occurred and corrugated undulations appeared, increasing the surface roughness of the specimen and leading to an increase in the coefficient of friction in the wear process. For both aged PE-UHMW and PE-UHMW/GO, the primary wear mechanism was fatigue and abrasive wear.

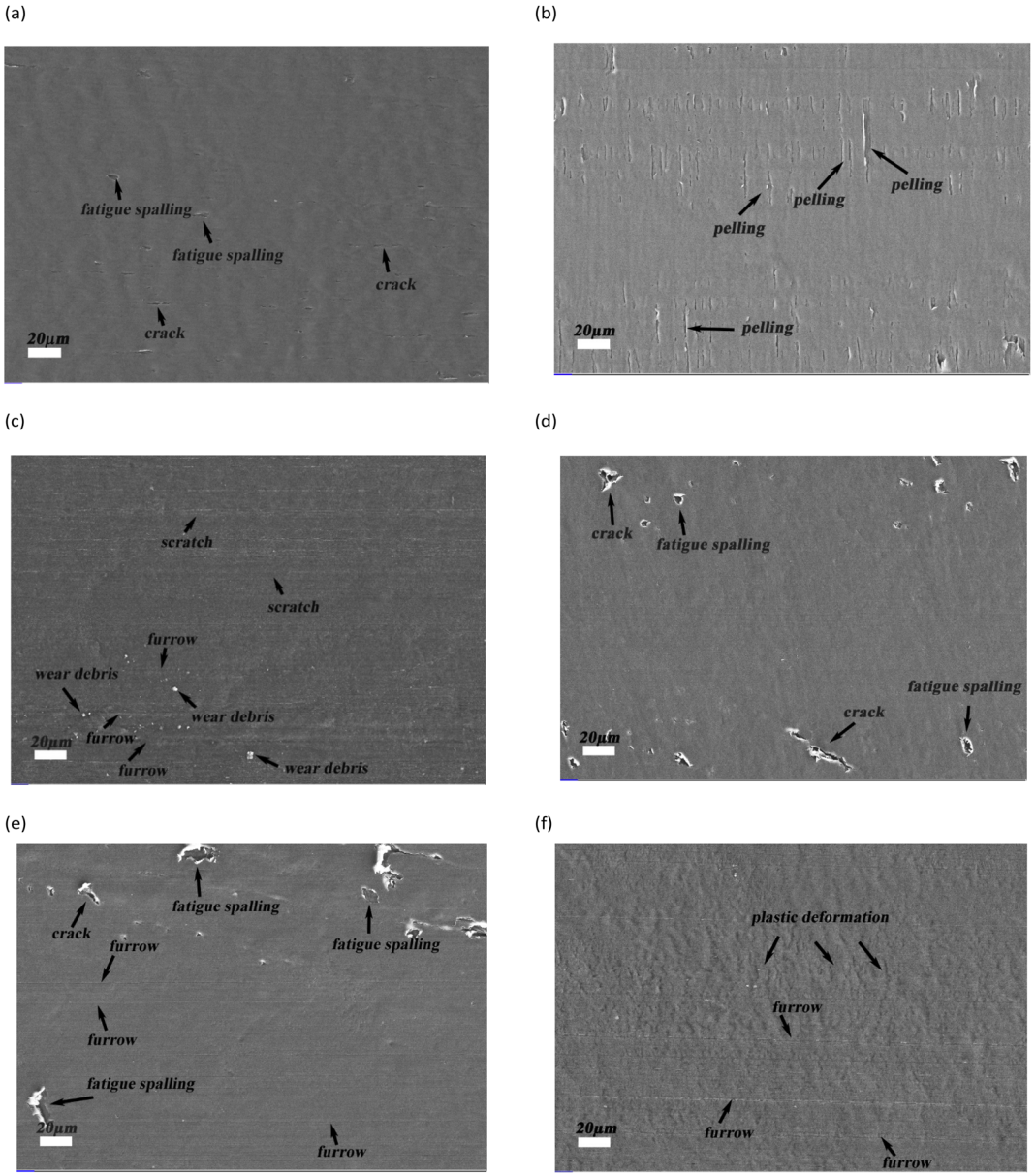

Fig. 6 SEM images (1000× magnification) of the worn surface of different treated PE-UHMW and PE-UHMW/GO composites under water lubrication: (a) PE-UHMW, (b) PE-UHMW/GO, (c) irradiated PE-UHMW, (d) irradiated PE-UHMW/GO, (e) aged PE-UHMW, (f) aged PE-UHMW/GO.

3.7 Irradiation-induced enhancement mechanism

The gamma irradiation technique significantly improved the compressive strength, yield strength and wear resistance of the PE-UHMW/GO composites by enhancing the interaction between GO and PE-UHMW. This enhancement was attributed to the reinforcement of the interface bonding force between GO and the PE-UHMW matrix.

According to the reports in the literature,[14,15,31,37] when the PE-UHMW/GO composites were exposed to irradiation, the free radicals and chemical bonds were generated. The irradiation enhancement mechanism is elucidated in Fig. 7.

As depicted in Fig. 7, the gamma irradiation process induced the fracture of numerous oxygen-containing functional groups of GO, particularly the C–O bonds,[38] leading to the reduction of GO to rGO. Simultaneously, irradiation cleaved C–H and C–C bonds in PE-UHMW, generating free radicals.[22] These free radicals underwent recombination, forming crosslinking, including H-crosslinking (Fig. 7(c)) and Y-crosslinking[1] (Fig. 7(d)). The generated radicals and PE-UHMW molecules could react with rGO, resulting in the formation of C–C chemical bonds.[37] This interaction enhanced the interface bonding force between GO and the PE-UHMW matrix, thereby improving the performance of the composites materials.

In contrast, non-irradiated PE-UHMW/GO composites exhibited interactions between GO and PE-UHMW primarily through weak van der Waals forces. The irradiation-induced modifications, including the reduction of GO and the

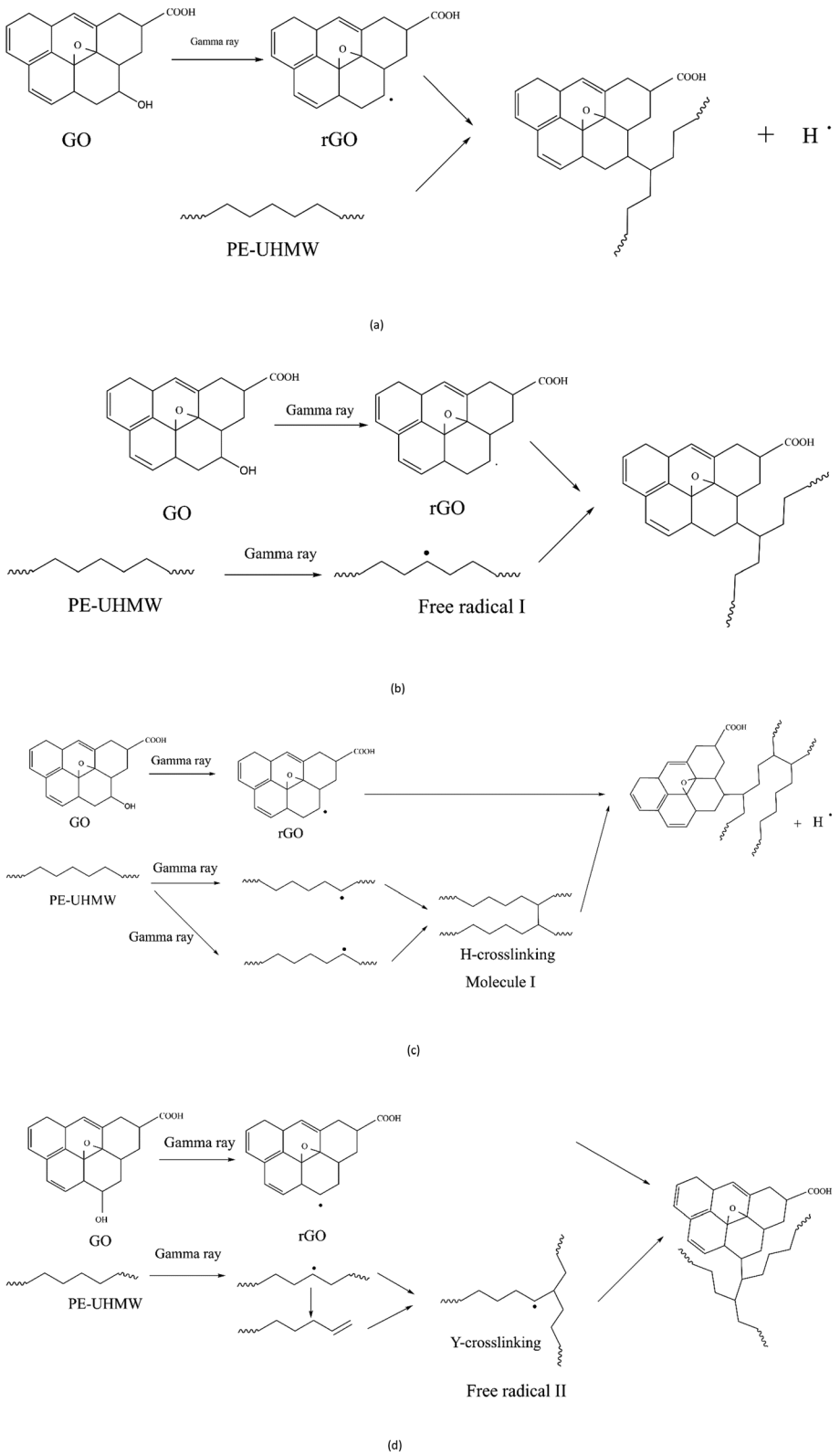

Fig. 7 Mechanistic insights into irradiation-induced enhancement *via* free radical and molecular interactions with rGO in the composite. (a) The reaction pathway of the PE-UHMW molecule and rGO. (b) The reaction pathway of the free radical I and rGO. (c) The reaction path of the molecule I and rGO. (d) The reaction pathway of the free radical II and rGO.

formation of crosslinking, led to the establishment of stronger intermolecular bonds within the composite material. Consequently, the tribological and compressive properties of the PE-UHMW/GO composites were markedly enhanced by irradiation.

4. Conclusions

In this investigation, the PE-UHMW/GO composites were prepared by ball milling and subsequently hot pressing. The composites were subjected to gamma irradiation and accelerated aging, respectively. This study investigated the water absorption, mechanical, and tribological properties of these composites. The main conclusions are shown as follows.

GO, enriched with the oxygen-containing functional groups, exhibited better dispersion in the PE-UHMW matrix. Aging had a considerable impact on water absorption, whereas irradiation had a minimal effect. Irradiation significantly enhanced the mechanical and tribological properties of the composites. The irradiated composites exhibited a 6.11% increase in compressive strength and a 25.72% increase in yield strength. Irradiation improved wear resistance and reduced the friction coefficient of the composites under water lubrication. Conversely, the process of aging led to the deterioration of these properties due to oxidative degradation. The aged composites showed a decrease of 14.74% in compressive strength and 21.12% in yield stress compared to the irradiation composites. The aging process also led to an increase in the friction coefficient and a decrease of the wear resistance in the composites. The main wear mechanism for the irradiated composites was fatigue wear, while for aged composites, it involved both abrasive wear and fatigue wear. The irradiation enhancement mechanism was attributed to the formation of the strong interracial binding force between GO and PE-UHMW during the irradiation process.

However, there are still some shortcomings in this study. Firstly, the impact strength of these composites was not investigated. Secondly, the characterization of wear particles was not studied. Finally, the effect of different normal loads on the friction were not investigated. Therefore, further research is required to enhance our understanding of PE-UHMW/GO composites so that they can be used for artificial joint materials in the future.

Conflicts of interest

There are no conflicts to declare.

Acknowledgements

The authors gratefully acknowledge the support of the Jiangsu Natural Science Foundation (No. BK20201142) and Jiangsu Provincial Vocational Education Teaching Reform Research Project (No. ZYB674).

References

1 S. M. Kurtz, *UHMWPE Biomaterials Handbook: Ultra High Molecular Weight Polyethylene in Total Joint Replacement and Medical Devices*, Academic press, 2009.
2 N. A. Patil, J. Njuguna and B. Kandasubramanian, *Eur. Polym. J.*, 2020, **125**, 109529.
3 M. M. Rahman, M. A. S. Biswas and K. N. Hoque, *Biotribology*, 2022, 100216.
4 S. Gürgen, *Polym. Degrad. Stab.*, 2022, **199**, 109912.
5 Z. Ahmed Baduruthamal, A. S. Mohammed, A. M. Kumar, M. A. Hussein and N. Al-Aqeeli, *Materials*, 2019, **12**, 3665.
6 Y. V. Dontsov, S. V. Panin, D. G. Buslovich and F. Berto, *Materials*, 2020, **13**, 2718.
7 P. Subhedar, D. Padmanabhan, R. Agrawal and G. Singh, *Mater. Today: Proc.*, 2023, DOI: **10.1016/j.matpr.2023.06.435**.
8 G. Yang, G. Meng, H. Gao and Q. Lin, *Polym. Compos.*, 2022, **43**, 3716–3730.
9 J. Xu, T. Han, C. Zhang and J. Luo, *Tribol. Int.*, 2023, 109142.
10 A. Chih, A. Ansón-Casaos and J. Puértolas, *Tribol. Int.*, 2017, **116**, 295–302.
11 E. Lorenzo-Bonet, M. Hernandez-Rodriguez, O. Perez-Acosta, M. De la Garza-Ramos, G. Contreras-Hernandez and A. Juarez-Hernandez, *Wear*, 2019, **426**, 195–203.
12 A. Kumar, J. Bijwe and S. Sharma, *Wear*, 2017, **378**, 35–42.
13 Y. Chen, Y. Qi, Z. Tai, X. Yan, F. Zhu and Q. Xue, *Eur. Polym. J.*, 2012, **48**, 1026–1033.
14 P. Lu, M. Wu, Z. Ni and G. Huang, *Polym. Bull.*, 2021, **78**, 5153–5164.
15 Z. Ni, W. Pang, G. Chen, P. Lu and S. Qian, *Russ. J. Appl. Chem.*, 2017, **90**, 1876–1882.
16 M. Traina and A. Pegoretti, *J. Nanopart. Res.*, 2012, **14**, 1–6.
17 W. Pang, Z. Ni, G. Chen, G. Huang, H. Huang and Y. Zhao, *RSC Adv.*, 2015, **5**, 63063–63072.
18 Z. Tai, Y. Chen, Y. An, X. Yan and Q. Xue, *Tribol. Lett.*, 2012, **46**, 55–63.
19 Y. An, Z. Tai, Y. Qi, X. Yan, B. Liu, Q. Xue and J. Pei, *J. Appl. Polym. Sci.*, 2014, **131**, 39640.
20 S. Suner, R. Joffe, J. Tipper and N. Emami, *Composites, Part B*, 2015, **78**, 185–191.
21 E. M. Brach del Prever, A. Bistolfi, P. Bracco and L. Costa, *J. Orthop. Traumatol.*, 2009, **10**, 1–8.
22 P. Bracco, L. Costa, M. P. Luda and N. Billingham, *Polym. Degrad. Stab.*, 2018, **155**, 67–83.
23 P. Bracco and E. Oral, *Clin. Orthop. Relat. Res.*, 2011, **469**, 2286–2293.
24 M. Martínez-Morlanes, P. Castell, P. J. Alonso, M. Martinez and J. Puértolas, *Carbon*, 2012, **50**, 2442–2452.
25 W. S. Hummers Jr and R. E. Offeman, *J. Am. Chem. Soc.*, 1958, **80**, 1339.
26 S. Mao, H. Pu and J. Chen, *RSC Adv.*, 2012, **2**, 2643–2662.
27 M. Terrones, O. Martín, M. González, J. Pozuelo, B. Serrano, J. C. Cabanelas, S. M. Vega-Díaz and J. Baselga, *Adv. Mater.*, 2011, **23**, 5302–5310.
28 L. Chen, Z. Chen, X. Tang, W. Yan, Z. Zhou, L. Qian and S. H. Kim, *Carbon*, 2019, **154**, 67–73.
29 S. Stankovich, R. D. Piner, S. T. Nguyen and R. S. Ruoff, *Carbon*, 2006, **44**, 3342–3347.
30 A. Rincón, R. Moreno, C. F. Gutiérrez-González, R. Sainz, M. D. Salvador and A. Borrell, *J. Eur. Ceram. Soc.*, 2016, **36**, 1797–1804.

31 G. Huang, Z. Ni, G. Chen, W. Pang and Y. Zhao, *Int. J. Polym. Anal. Charact.*, 2016, **21**, 417–427.
32 A. Gholampour, M. Valizadeh Kiamahalleh, D. N. Tran, T. Ozbakkaloglu and D. Losic, *ACS Appl. Mater. Interfaces*, 2017, **9**, 43275–43286.
33 L. Costa and P. Bracco, in *UHMWPE Biomaterials Handbook*, Elsevier, 2016, pp. 467–487.
34 J. Zhao, Y. Li, Y. Wang, J. Mao, Y. He and J. Luo, *RSC Adv.*, 2017, **7**, 1766–1770.
35 A. S. Mohammed and A. Bin Ali, *Tribol. Lett.*, 2016, **62**, 1–9.
36 H. R. Holgate, J. C. Meyer and J. W. Tester, *AIChE J.*, 1995, **41**, 637–648.
37 W. Duan, M. Wu, J. Han and Z. Ni, *RSC Adv.*, 2020, **10**, 4175–4188.
38 L. F. Dumée, C. Feng, L. He, F.-M. Allioux, Z. Yi, W. Gao, C. Banos, J. B. Davies and L. Kong, *Appl. Surf. Sci.*, 2014, **322**, 126–135.